Ecological Indicators 98 (2019) 568–574

Contents lists available at ScienceDirect

Ecological Indicators

journal homepage: www.elsevier.com/locate/ecolind

Estimating green biomass ratio with remote sensing in arid grasslands

Hongrui Ren[a,*], Guangsheng Zhou[b,*]

[a] Department of Geomatics, College of Mining Engineering, Taiyuan University of Technology, Taiyuan 030024, China
[b] Chinese Academy of Meteorological Sciences, Beijing 100081, China

ARTICLE INFO

Keywords:
Green biomass ratio
Arid grasslands
Remote sensing
Hyperspectral vegetation indices
Medium-infrared bands

ABSTRACT

It is difficult to estimate green biomass ratio (GBR), the ratio of green aboveground biomass to total aboveground biomass, using common broad-band vegetation indices in arid grasslands due to similar spectral features between bare soil and non-photosynthetic vegetation in near-infrared (NIR) and visible bands. We evaluated the performance of the broad-band RVI (ratio vegetation index), NDVI (normalized difference vegetation index), SAVI (soil-adjusted vegetation index), MSAVI (modified soil-adjusted vegetation index), OSAVI (optimized soil-adjusted vegetation index), $NDVI_{green}$ (green normalized difference vegetation index), CI (canopy index), and NCI (normalized canopy index) for GBR estimation in the desert steppe of Inner Mongolia, China. We also explored best narrow-band hyperspectral vegetation indices for GBR estimation using hyperspectral remotely sensed data and GBR measurements during 2009 and 2010 growing seasons in the desert steppe. Broad-band vegetation indices were not suitable for GBR estimation. The best narrow-band vegetation indices used reflectance at 2069 and 2042 nm; particular $1.5 \times (R_{2069} - R_{2042})/(R_{2069} + R_{2042} + 0.5)$. The index could partially overcome the influence of bare soil cover. It explained 68% of the variance of GBR and dramatically improved GBR estimation accuracy over common broad-band indices. More importantly, the accuracy was not affected by varying bare soil cover. Nevertheless, caution is required for the index application within varying growing seasons. The development of this index is an important resource for future spectral sensors that will permit GBR monitoring at regional scales in arid grasslands. Our results show that remote imagery can monitor GBR in the desert steppe and potentially in many arid grasslands.

1. Introduction

Green biomass ratio (GBR), the ratio of green aboveground biomass to total aboveground biomass (green plants, standing dead plants, and litter), is a very important variable of carbon cycles and ecosystem processes in grasslands. The ratio is used as a significant ecological indicator of grassland maturity and senescence and has been widely used to model vegetation dynamics (Herrmann and Schachtel, 2001; Zhang and Romo, 1994), photosynthesis (Tappeinner and Cernusca, 1998), pasture management (Garcia et al., 2003), and ecosystems (Teague and Foy, 2002). The traditional method of measuring GBR is to hand separate fractions that have been destructive sampled. This is expensive, time-consuming, and feasible only over small areas.

Remote sensing technology is a remarkably successful method for vegetation biophysical and biochemical parameter measures from local to global scales. Vegetation indices, such as RVI (ratio vegetation index; Jordan, 1969), NDVI (normalized difference vegetation index; Rouse et al., 1974), SAVI (soil-adjusted vegetation index; Huete, 1988), MSAVI (modified soil-adjusted vegetation index; Qi et al., 1994), and OSAVI (optimized soil-adjusted vegetation index; Rondeaux et al., 1996), derived from red and near-infrared (NIR) bands are closely related to green vegetation biomass (Ren et al., 2018a,b), green vegetation leaf area index (Liu et al., 2011), green vegetation cover (Jiapaer et al., 2011), and biochemical components (Wang et al., 2013) in grasslands. Nevertheless, few studies have explored the capacity of remote sensing data to estimate GBR in grasslands.

In a field study, Gianelle and Vescvo (2007) explored the potential of vegetation indices derived from visible and NIR bands for GBR estimation in the Italian Alps and New Zealand grasslands. Their results showed that green normalized difference vegetation index ($NDVI_{green}$) (Gitelson et al., 1996) derived from NIR and green bands, performed well for GBR estimation. The performance of $NDVI_{green}$ was also confirmed for aircraft using ASPIS (Advanced SPectroscopic Imaging System) aircraft sensor imagery and satellite using IRS (Indian Remote Sensing) satellite sensor imagery (Vescovo and Gianelle, 2006). To explore the potential of medium-infrared (MIR) bands, Vescovo and

* Corresponding authors at: Department of Geomatics, College of Mining Engineering, Taiyuan University of Technology, No. 79, West Yingze Street, Taiyuan 030024, China (H. Ren). Chinese Academy of Meteorological Sciences, No. 46, Zhongguancun South Street, Haidian District, Beijing 100081, China (G. Zhou).
E-mail addresses: renhongrui@tyut.edu.cn (H. Ren), zhougs@cma.gov.cn (G. Zhou).

https://doi.org/10.1016/j.ecolind.2018.11.043
Received 7 August 2018; Received in revised form 9 November 2018; Accepted 15 November 2018
Available online 22 November 2018
1470-160X/

Gianelle (2008) proposed the MIR/green ratio (CI, Canopy Index) and normalized difference between MIR and green bands (NCI, Normalized Canopy Index) to estimate GBR in grasslands using IRS and SPOT 5 (Systeme Probatoire d'Observation de la Terre 5) images. Their results suggested that CI and NCI had potential to estimate GBR in grasslands in the Italian Alps region.

To test the performance of $NDVI_{green}$, CI, and NCI in arid grasslands, we have previously tested the accuracy of GBR estimation in desert steppe of Xilingol League, Inner Mongolia, China with IRS and SPOT 5 data. Unexpectedly, $NDVI_{green}$, CI, and NCI accounted for only 2%, 6%, and 6% of the variability in measured GBR (unpublished data). This was much lower than that reported by Vescovo and Gianelle (2006, 2008). We suggested that these vegetation indices might lose their ability to estimate GBR due to higher soil cover in the desert steppe. In sparse canopy environments, the significant influence of bare soil sharply weakens spectral features of photosynthetic vegetation (green plants). This is the high reflectance in NIR bands and strong chlorophyll absorption in red bands. Moreover, soil and non-photosynthetic vegetation (standing dead plants and litter) are spectrally similar in NIR and visible bands and differ only in reflectance magnitude at a given wavelength (Baird and Baret, 1997; Ren and Zhou, 2012; Ren et al., 2018a,b).

In the previous two decades, hyperspectral data have shown great potential to describe biophysical and biochemical parameters. The important advantage that hyperspectral data offers is the ability to identify optimal bands for maximizing the narrow-band sensitivity of vegetation indices for specific vegetation parameters. It also permits *ad hoc*, narrow-band vegetation indices that are closely related to specific vegetation parameters. As shown in many studies of green vegetation biomass, leaf area index, and cover estimation in arid grasslands, narrow-band vegetation indices could partially overcome the influence of bare soil and dramatically improve estimation accuracy across broad-band vegetation indices (Boschetti et al., 2007; Elvidge and Chen, 1995; Li, 2008; Ren et al., 2011). Nevertheless, very few studies have been conducted to explore best narrow-band vegetation indices for estimating GBR in arid grasslands.

The objectives of this study were to: (1) evaluate the performance of broad-band vegetation indices (RVI, NDVI, SAVI, MSAVI, OSAVI, $NDVI_{green}$, CI, and NCI) for GBR estimation in arid grasslands, (2) identify the best, narrow-band vegetation index for estimating GBR in arid grasslands, and (3) analyze the sensitivity of the best narrow-band vegetation index to bare soil cover and growth seasons in arid grasslands. To achieve these objectives, field hyperspectral data and corresponding vegetation parameters were measured in the desert steppe of Inner Mongolia, the typical representative of arid grasslands in China.

2. Materials and methods

2.1. Study area

Field surveys were conducted at the Sonid Zuoqi temperate desert steppe ecosystem research station (44°05′19″N, 113°34′20″E, 972 a.s.l.) where grazing and other anthropogenically regulated activities had been prevented. The study area is characterized by a typical arid continental climate. Precipitation is the major factor limiting vegetation growth and vegetation productivity. According to long-term meteorological data from 1956 to 2009 at the weather station in Sonid Zuoqi, mean annual precipitation (MAP) ranges from 96.3 to 321.7 mm ($\bar{x}$ = 191.9 mm). Nevertheless, more than 80% of annual precipitation falls during the growing season months (from May to September). Vegetation in the study area is dominated by *Stipa klemenzii* Roshev. with other dominant species; *Cleistogenes squarrosa (Trin.)* Keng, *Caragana microphylia* Lam., *Agropyron desertorum (Fisch.)* Schult., and *Artemisia frigida* Willd.Sp.Pl. The soil in the study area belongs to argids (suborder) of aridisols (order).

2.2. Data collection

Field hyperspectral data and vegetation parameter measurements were collected during the growing seasons of 2009 (13–17 May, 6–11 June, 11–17 July, 6–13 August, 16–20 September) and 2010 (23–30 August). For each hyperspectral and vegetation measurement in 2009, 24 field plots (0.5 m × 0.5 m) and in 2010, 38 field plots (0.5 m × 0.5 m) were randomly selected. In total, 158 plots (120 in 2009 and 38 in 2010) were selected to measure hyperspectral data and vegetation parameters. The distance between the plots was about a few hundred meters. The selected plots can represent the study area well in the variances of GBR without autocorrelation (Yan et al., 2012). All plots were geo-located using a differential GPS (global positioning system) with the accuracy of ± 5 m to avoid re-measurement in the plots in different field surveys.

Field hyperspectral data measurements were conducted using an ASD (Analytical Spectral Device) portable spectrometer (Inc., Boulder, Colorado, USA) from 11:30 to 14:00 (China Standard Time) in sunny days with no wind and clouds. The spectrometer can acquire reflectance in 2151 bands from 350 nm to 2500 nm with spectral resolution of 1 nm. During measurements, the spectrometer, with a FOV (field of view) of 25°, was placed approximately 1.2 m above the ground at nadir position. This allowed the coverage of an area with a diameter of about 0.5 m. To accurately capture the spectral features, thirty hyperspectral measurements were made for each plot. Spectra for each plot were averaged to offer a single spectrum for the entire plot. Before the spectra measurement for each plot, the radiance of a calibrate white standard panel comprised of $BaSO_4$ was also measured to normalize the canopy spectra measurements.

Following hyperspectral measurements, living vascular plants and standing dead plants within each plot were clipped at the ground surface, and litter within each plot was also collected. All plant material was divided manually into green (living vascular plants) and senesced (standing dead plants and litter) tissue. Fresh weight of green and senesced plants was recorded using an electronic balance with a sensitivity of 0.01 g. The plants were oven-dried to a constant mass at 65 °C for 48 h and weighed to the nearest 0.01 g. Green biomass ($g\,m^{-2}$) and senesced biomass ($g\,m^{-2}$) for each plot were derived by dividing the dried weight of green and senesced tissue by the area of the plot (0.5 m × 0.5 m), respectively. GBR for each plot was calculated by dividing green biomass by total biomass (green biomass + senesced biomass). In the measurements, three senesced plant samples were damaged and in total 155 plant samples were remained for the analysis in this study.

2.3. Broad-band vegetation indices

The RVI, NDVI, SAVI, MSAVI, OSAVI, $NDVI_{green}$, CI, and NCI were determined as follows:

$$RVI = \frac{R_{NIR}}{R_{red}} \quad (1)$$

$$NDVI = \frac{R_{NIR} - R_{red}}{R_{NIR} + R_{red}} \quad (2)$$

$$SAVI = \frac{1.5\times(R_{NIR} - R_{red})}{R_{NIR} + R_{red}+0.5} \quad (3)$$

$$MSAVI = 0.5 \times ((2 \times R_{NIR} + 1) - \sqrt{(2\times R_{NIR} + 1)^2 - 8\times (R_{NIR} - R_{red})}) \quad (4)$$

$$OSAVI = \frac{R_{NIR} - R_{red}}{R_{NIR} + R_{red}+0.16} \quad (5)$$

$$NDVI_{green} = \frac{R_{NIR} - R_{green}}{R_{NIR} + R_{green}} \quad (6)$$

$$CI = R_{MIR} - R_{green} \quad (7)$$

$$NCI = \frac{R_{MIR} - R_{green}}{R_{MIR} + R_{green}} \quad (8)$$

where R_{NIR} is the reflectance at NIR band, R_{red} is the reflectance at red band, R_{MIR} is the reflectance at MIR band, and R_{green} is the reflectance at green band. In this study, the reflectance at green, red, NIR, and MIR bands was obtained by spectral resampling from ASD Fieldspec channels to TM sensor (TM 2, 3, 4, and 5). The resampling was performed using the spectral resampling routine available on ENVI4.3 software (Research Systems, Inc.).

Unlike green vegetation biomass and leaf area index (LAI), no saturation effect occurs in vegetation indices above a certain GBR values in grasslands (Vescovo and Gianelle, 2006). Our results in this study also showed that significant improvement over non-linear regression was observed for linear regression (not shown). Thus, using all data (n = 155), linear regression models were used to evaluate the performance of these broad-band vegetation indices for GBR estimation in the desert steppe of Inner Mongolia. The performance of these vegetation indices was evaluated by the R^2 (coefficients of determination) and RMSECV (root mean square error of leave-one-out cross validation).

2.4. Narrow-band vegetation indices

In the study, we selected two widely used vegetation indices models: normalized difference index (NDI) and soil-adjusted normalized difference index (S-NDI), which were determined as:

$$NDI = \frac{R_i - R_j}{R_i + R_j} \quad (9)$$

$$S\text{-}NDI = \frac{1.5\times(R_i - R_j)}{R_i + R_j + 0.5} \quad (10)$$

where R_i is the reflectance at band i and R_j is the reflectance at band j with $i \neq j$. The two indices were calculated from all band combinations in the spectral range (350–2500 nm) to identify best narrow-band vegetation indices for estimating GBR.

The GBR data set (n = 155) from this study was randomly split into training data (n = 102) and test data (n = 53). Training data were used to identify the best narrow-band vegetation indices, and test data were used to validate the best narrow-band indices. GBR values have consistent statistical characteristics for both data sets (Table 1). This suggested that GBR data were properly partitioned. GBR varied from 0.256 to 0.985 ($\bar{x}$ = 0.579). High variation ensures that the regression models between GBR and vegetation indices were as close to real as possible.

Similarly, we used linear regressions to explore which two-band combinations were more sensitive to GBR. The narrow-band combinations for these narrow-band vegetation indices were identified by R^2. Using the training data, the regression model estimation accuracies of the best narrow-band vegetation indices were evaluated by R^2 and RMSECV. The validation of these regression models was performed using the test data. The validation performance was assessed by R^2, RMSE and rRMSE (relative RMSE), expressed as a percentage.

Although it was not the primary objective of this study, we further explored the performance of the best narrow-band vegetation indices for GBR estimation using simulated Hyperion and AVIRIS hyperspectral data in Discussion section. Hyperion and AVIRIS are the representative of first-generation space-borne and airborne hyperspectral sensors respectively; both with high spectral resolution images (~10 nm). Our simulations were performed with spectral resampling routine available on ENVI 4.3 software (Research Systems, Inc.). A Gaussian response function was set for Hyperion and AVIRIS because spectral response functions were not available.

Table 1
Statistics of GBR for model training and test data.

Data	n	Mean	Standard deviation	Minimum	Maximum
All data	155	0.579	0.135	0.256	0.985
Training	102	0.582	0.138	0.256	0.985
Test	53	0.573	0.130	0.343	0.946

Table 2
Linear regression analyses between GBR and broad-band vegetation indices. Y represents GBR, and x represents broad-band vegetation index.

Vegetation index	Regression model	R^2	RMSECV	P
RVI	y = 0.16x + 0.34	0.02	0.134	> 0.05
NDVI	y = 0.51x + 0.48	0.02	0.134	> 0.05
SAVI	y = 1.28x + 0.41	0.07	0.131	> 0.05
MSAVI	y = −1.14x − 0.39	0.09	0.129	> 0.05
OSAVI	y = −0.86x − 0.44	0.04	0.132	> 0.05
$NDVI_{green}$	y = 1.01x + 0.26	0.04	0.132	> 0.05
CI	y = −0.86x + 0.94	0.04	0.132	> 0.05
NCI	y = −0.14x + 0.92	0.05	0.132	> 0.05

3. Results

3.1. Performance of broad-band vegetation indices

RVI, NDVI, SAVI, MSAVI, and OSAVI, widely used to estimate green vegetation biomass, cover, and leaf area index in arid grasslands, cannot be used to estimate GBR in arid grasslands (Table 2). All regression models based on the broad-band vegetation indices had low R^2 (< 0.1) and high RMSECV (0.129–0.134). No regression model was significant (P > 0.05).

According to the works of Gianelle and Vescvo (2007) and Vescovo and Gianelle (2006, 2008), the broad-band $NDVI_{green}$, CI, and NCI, specialized for GBR estimation in grasslands, should have good performance for GBR estimation in this study. Nevertheless, these vegetation indices accounted for only 5% of the variability in measured GBR (Table 2), a very poor performance for GBR estimation in arid grasslands.

3.2. Best narrow-band NDI and S-NDI

The R^2 derived from linear regressions of GBR using training data against all narrow-band NDI [i, j] and S-NDI [i, j] are shown in Figs. 1 and 2. The intersection of each two-band combination corresponded to an R^2 value derived from linear regression of GBR against narrow-band vegetation index computed from the reflectance in the two bands [i, j]. The values of R^2 vary from 0.0 to 0.7. This suggested significant range in the strength of the relationship between GBR and selected vegetation indices.

Similar correlation patterns with the similar R^2 values were observed for NDI and S-NDI against GBR (Figs. 1 and 2). Nevertheless, a very large segment of all narrow-band combinations showed poor accuracy (R^2 < 0.6) for GBR estimation. The narrow-band combinations with higher R^2 (> 0.6, P < 0.001) were located entirely in the MIR range. The best narrow-band combination with the highest R^2 was determined according the value of R^2 in the plots. The best band combination for NDI and S-NDI was at 2069 nm and 2042 nm.

Both regression models using training data to compare GBR and best NDI and S-NDI were statistically significant at P < 0.001 (Figs. 3(a) and 4(a)). The best NDI [2069, 2042] explained about 67.7% of the variation in the GBR and yielded a RMSECV value of 0.079. Compared to NDI [2069, 2042], S-NDI [2069, 2042] yielded slightly higher R^2 (0.688) and slightly lower RMSECV (0.077) with the training data.

The validation of NDI [2069, 2042] and S-NDI [2069, 2042] was conducted using the test data. Compared to NDI [2069, 2042] (R^2 = 0.624, RMSE = 0.08, rRMSE = 14%, P < 0.001) (Fig. 3(b)), S-

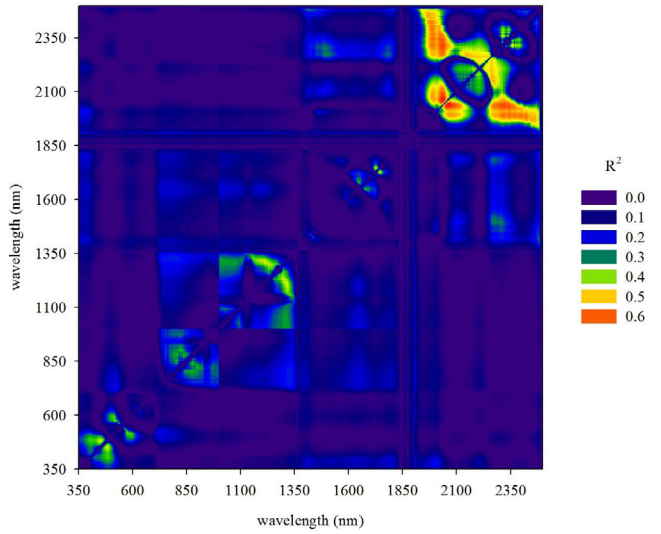

Fig. 1. Contour chart showing R^2 from linear regression models between NDI obtained from all narrow-band combinations and GBR.

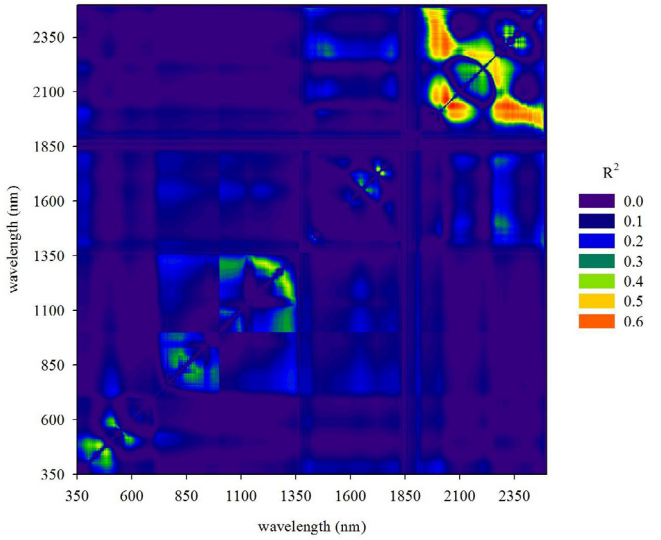

Fig. 2. Contour chart showing R^2 from linear regression models between S-NDI obtained from all narrow-band combinations and GBR.

NDI [2069, 2042] had slightly higher R^2 (0.633), slightly lower RMSE (0.078), and slightly lower rRMSE (13.6) using the test data (Fig. 4(b)). These results suggested that, NDI [2069, 2042] and S-NDI [2069, 2042] could be used to estimate GBR with better accuracy in arid grasslands. We retained S-NDI [2069, 2042] for the rest of the analysis due to its slightly higher accuracy.

3.3. Effects of bare soil cover and growing seasons

The linear regression of S-NDI [2069, 2042] against GBR was built using all data (n = 155) (Figs. 5 and 6). Due to soil-vegetation spectral mixing in the study area, bare soil cover is a potential source of variation of the relationship between vegetation indices and GBR (Fig. 5). Nevertheless, it was obvious that the fractional cover of bare soil did not stand out as a factor explaining the scatter of the relationship between GBR and S-NDI [2069, 2042]. This suggests the stability of the relationship between GBR and S-NDI [2069, 2042] through varying vegetation cover.

Although the data from the same growing seasons did not form distinct cluster, there were clear patterns (Fig. 6). These depends on

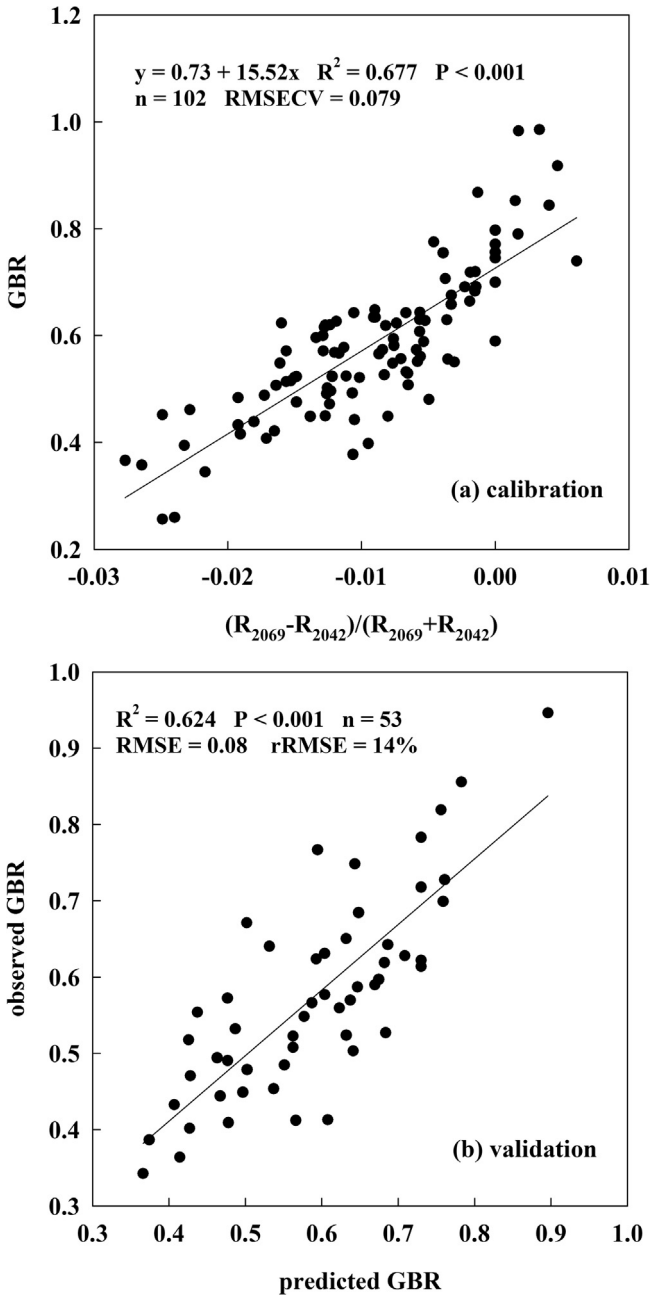

Fig. 3. Training (a) and test (b) of best narrow-band NDI for GBR estimation.

when the field data were collected, particularly for the data collected in August 2010 when lower GBR and lower S-NDI [2069, 2042] were observed. In addition, a few data collected in June 2009 departed from the regression line. Thus, the regression model tends to slightly underestimate the GBR in June 2009. These results suggested that the accuracy of the newly index for GBR estimation may vary within growing seasons in arid grasslands.

4. Discussion

Because of the strong influence of bare soil reflectance, it is difficult to quantify GBR in arid grasslands using common broad-band vegetation indices (Table 2). The newly developed hyperspectral narrow-band index in this study, $1.5 \times (R_{2069} - R_{2042})/(R_{2069} + R_{2042} + 0.5)$, yielded the best accuracy for GBR estimation in the desert steppe of Inner Mongolia. The newly developed index showed far better estimation accuracy than broad-band vegetation indices. We concluded that,

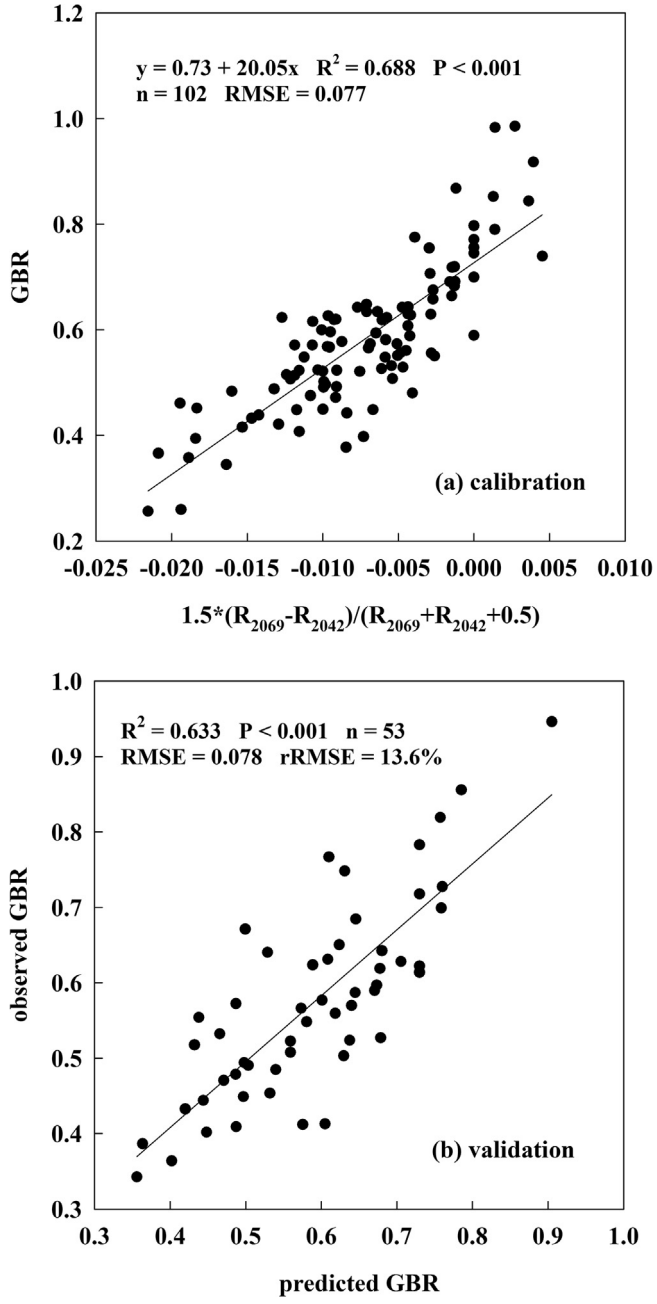

Fig. 4. Training (a) and test (b) of best narrow-band S-NDI for GBR estimation.

the index can partially overcome the influence of bare soil and improve GBR estimation accuracy over broad-band indices in arid grasslands.

The good performance of the newly developed index for GBR estimation in arid grasslands was attributed to the sensitivity of canopy reflectance to water content in the MIR region (2069 nm and 2042 nm in the index). An increase in vegetation water content can cause a decrease (absorption) in MIR bands reflectance (Vescovo and Gianelle, 2008). The key of the variances of GBR is exactly the variances of vegetation water content. Thus, the sensitivity appears to be a valid approach for GBR estimation in arid grasslands. Although the use of MIR spectral region was suggested many years ago, spectral indices using MIR spectral region have probably been under-unitized (Everiti et al., 1989).

Compared with narrow-band NDI [2069, 2042], the newly developed S-NDI [2069, 2042], incorporating a soil-adjusted factor (0.5) into narrow-band NDI [2069 2042], showed only a slight improvement for

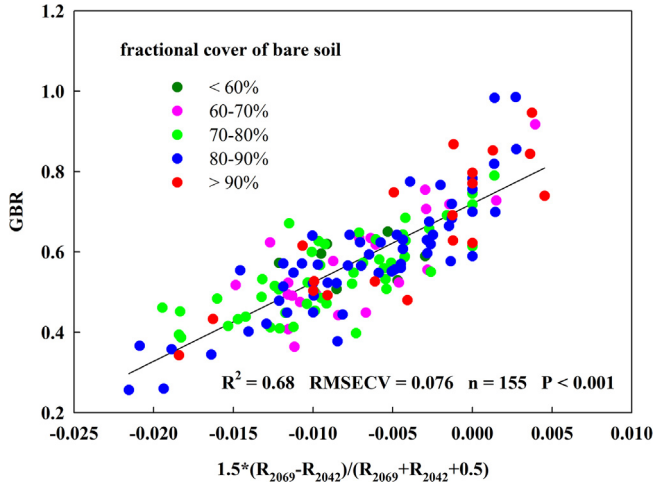

Fig. 5. Effect of fractional cover of bare soil on the relationship between GBR and S-NDI [2069, 2042].

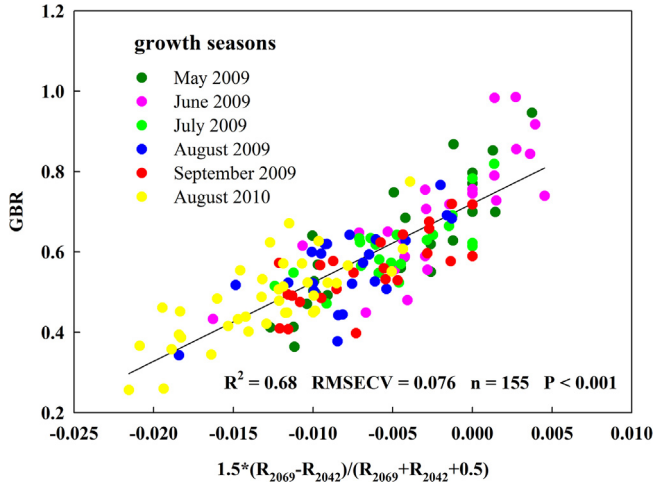

Fig. 6. Effect of growing seasons on the relationship between GBR and S-NDI [2069, 2042].

GBR estimation in the desert steppe of Inner Mongolia. This may be attributed to very low vegetation cover in the study area. We speculated that, in sparse canopy environments, vegetation spectral information was faint, and the soil-adjusted factor had limited capacity to remove soil signal and intensify vegetation signal. This was also observed in other studies of green biomass estimation using remotely sensed data in arid grasslands (Ren et al., 2011; Ren and Feng, 2015).

Although the newly developed narrow-band index could cope with effect of varying bare soil cover, some caution has to be expressed in the use of the new index in arid grasslands due to its sensitivity to growing seasons (Fig. 6). We ascribe this sensitivity to varying vegetation water content among different growing seasons. It is necessary to assess effect of growing seasons on the performance of the index for estimating GBR in other arid grasslands.

Although there are currently no space-borne and airborne sensors that are capturing narrow band reflectance used in this index, its development through field hyperspectral data is important to determine whether it is dependent on specific spectral resolution and exportable to airborne and space-borne sensors. Our results provide reference to planned satellite sensors that will allow this newly developed index to be calculated.

We further explored the performance of S-NDI [2069, 2042] for GBR estimation using simulated Hyperion and AVIRIS hyperspectral data. In the calculation of S-NDI [2069, 2042] using Hyperion data, the

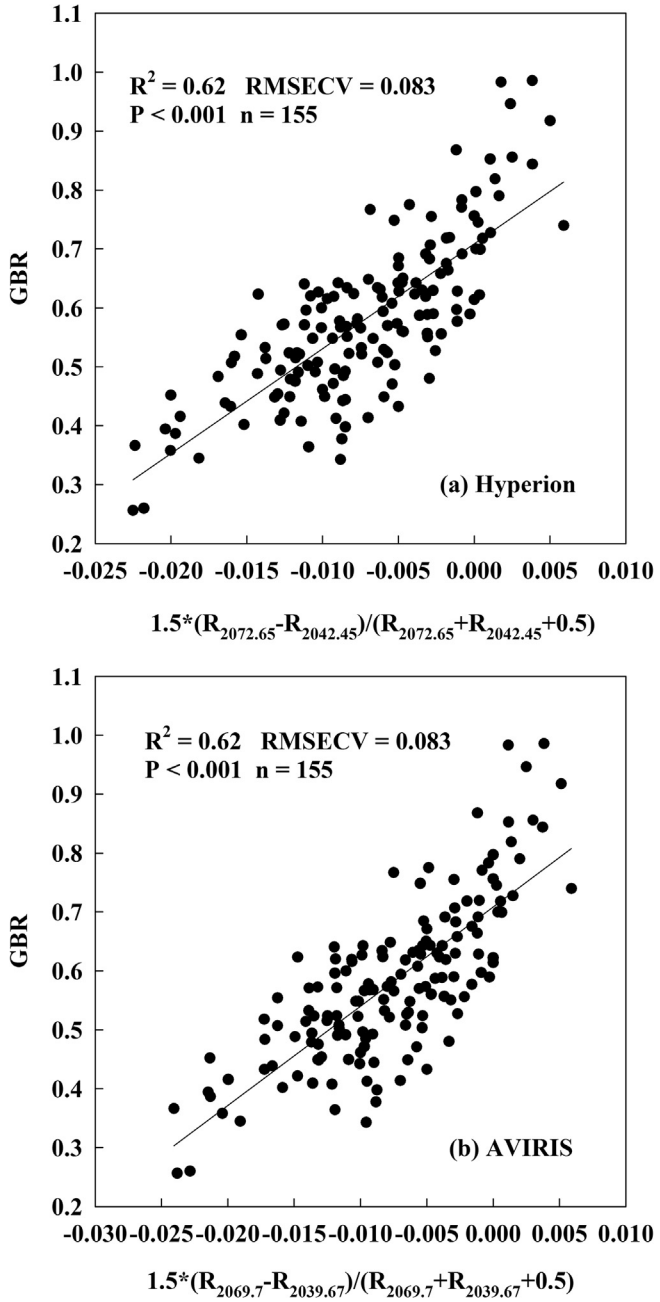

Fig. 7. Linear regression analyses between GBR and S-DNI [2072.65, 2042.45] using simulated Hyperion data (a) and S-NDI [2069.7, 2039.67] using simulated AVIRIS data (b).

reflectance at 2069 nm was replaced by that at Band 192 (centered at 2072.65 nm), and the reflectance at 2042 nm was replaced by that at Band 189 (centered at 2042.45 nm). In the calculation using simulated AVIRIS data, the reflectance at 2069 nm was replaced by that at Band 180 (centered at 2069.7 nm), and the reflectance at 2042 nm was replaced by that at Band 177 (centered at 2039.67 nm).

Regression models showed slightly lower R^2 and higher RMSECV compared with that based on field hyperspectral data (Fig. 7) and our new index could explain 62% of the variance in GBR. S-DNI calculated from Hyperion and AVIRIS data may be fairly reliable predictors of GBR. Nevertheless, compared with pixel size of these hyperspectral data (Hyperion: 30 m × 30 m; AVIRIS: 20 m × 20 m), the measured plots of field hyperspectral data were much smaller. The atmospheric environments of space-borne and airborne hyperspectral data were also different from that of the plot-scale field measurements. Therefore, further studies need to be conducted to evaluate the performance of the newly developed vegetation index for GBR estimation using real space-borne and airborne hyperspectral data in arid grasslands.

5. Conclusions

The common broad-band RVI, NDVI, SAVI, MSAVI, OSAVI, $NDVI_{green}$, CI, and NCI were not reliable indicators of GBR in arid grasslands with high bare soil cover due to similar spectral features between bare soil and non-photosynthetic vegetation in the NIR and visible bands. The newly developed hyperspectral narrow-band spectral index, $1.5 \times (R_{2069} - R_{2042})/(R_{2069} + R_{2042} + 0.5)$, dramatically improved estimation accuracy over these broad-band vegetation indices and can be used to estimate GBR with good accuracy and robustness in arid grasslands. The performance of the newly developed index was not affected by varying bare soil cover. Nevertheless, we found the sensitivity of the index to growing seasons, implying that the estimation accuracy of the index may vary within growing seasons in arid grasslands.

The newly developed vegetation index could provide information for future space-borne and airborne hyperspectral sensors that can allow this narrow-band vegetation index to be calculated and subsequent estimation of GBR at regional scales in arid grasslands. We speculated that the newly developed vegetation index calculated from Hyperion and AVIRIS sensors may performed well. Future research is necessary to estimate GBR in arid grasslands with the index using real Hyperion and AVIRIS hyperspectral data.

Acknowledgments

The research was supported by Natural Science Foundation of Shanxi (201701D121120).

References

Baird, F., Baret, F., 1997. Crop residue estimation using multiband reflectance. Remote Sens. Environ. 59, 530–536.
Boschetti, M., Bocchi, S., Brivio, P.A., 2007. Assessment of pasture production in the Italian Alps using spectrometric and remote sensing information. Agric. Ecosyst. Environ. 118, 267–272.
Elvidge, C.D., Chen, Z.K., 1995. Comparison of broad-band narrow-band red and near-infrared vegetation index. Remote Sens. Environ. 54, 38–48.
Everiti, J.H., Escobar, D.E., Richardson, A.J., 1989. Estimating grassland phytomass production with near-infrared and mid infrared spectral variables. Remote Sens. Environ. 30, 257–261.
Garcia, F., Carrere, P.J., Soussana, F., Baumont, R., 2003. How do severity and frequency of grazing affect sward characteristics and the choices of sheep during the grazing season? Grass Forage Sci. 58, 138–150.
Gianelle, D., Vescovo, L., 2007. Determination of green herbage ratio in grasslands using spectral reflectance. Methods and ground measurements. Int. J. Remote Sensing 28, 931–942.
Gitelson, A.A., Kaufman, Y.J., Merzlyak, M.N., 1996. Use of a green channel in remote sensing of global vegetation from EOS-MODIS. Remote Sens. Environ. 58, 289–298.
Herrmann, A., Schachtel, G.A., 2001. OSYAQ, an organ-specific growth model for forage grasses. Grass Forage Sci. 563, 268–284.
Huete, A.R., 1988. A soil-adjusted vegetation index (SAVI). Remote Sens. Environ. 25, 295–309.
Jiapaer, G.L., Chen, X., Bao, A.M., 2011. A comparison of methods for estimating fractional vegetation cover in arid regions. Agric. Forest Meteorol. 151, 1698–1710.
Jordan, C.F., 1969. Derivation of leaf-area index from quality of light on the forest floor. Ecology 50, 663–666. Remote Sens. Environ. 48, 119–126.
Li, X.S., 2008. Quantitive Retrieval of Sparse Vegetation Cover in Arid Regions Using Hyperspectral Data. Chinese Academy of Forestry, Beijing.
Liu, Y.B., Ju, W.M., Zhu, G.L., Chen, J.M., Xing, B.L., Zhu, J.F., Zhou, Y.L., 2011. Retrieval of leaf area index for different grasslands in Inner Mongolia prairie using remote sensing data. Acta Ecol. Sin. 31, 5159–5170.
Qi, J., Chehbouni, A., Huete, A.R., Kerr, Y.H., Sorooshian, S., 1994. A modified soil adjusted vegetation index. Remote Sens. Environ. 48, 119–126.
Ren, H.R., Feng, G.R., 2015. Are soil-adjusted vegetation indices better than soil-unadjusted vegetation indices for above-ground green biomass estimation in arid and semi-arid grasslands? Grass Forage Sci. 70, 611–619.
Ren, H.R., Zhou, G.S., Zhang, X.S., 2011. Estimation of green aboveground biomass of desert steppe in Inner Mongolia based on red-edge reflectance curve area method. Biosyst. Eng. 109, 385–395.
Ren, H.R., Zhang, B., Guo, X.L., 2018a. Estimation of litter mass in nongrowing seasons in

arid grasslands using MODIS satellite data. Eur. J. Remote Sens. 51, 222–230.
Ren, H.R., Zhou, G.S., 2012. Estimating senesced biomass of desert steppe in Inner Mongolia using field spectrometric data. Agric. Forest Meteorol. 161, 66–71.
Ren, H.R., Zhou, G.S., Zhang, F., 2018b. Using negative soil adjustment factor in soil-adjusted vegetation index (SAVI) for aboveground living biomass estimation in arid grasslands. Remote Sens. Environ. 209, 439–445.
Rondeaux, G., Steven, M., Baret, F., 1996. Optimization of soil-adjusted vegetation indices. Remote Sens. Environ. 55, 95–107.
Rouse, J.W., Hass, R.H., Schell, J.A., Deering, D.W., 1974. Monitoring vegetation systems in the Great Plains with ERTS. In: Freden, S.C., Mercanti, E.P., Becker, M.A. (Eds.), Third ERTS Symposium. NASA SP-351 I, Washington, DC, pp. 309–317.
Tappeinner, U., Cernusca, A., 1998. Model simulation of spatial distribution of photosynthesis in structurally differing plant communities in the Central Caucasus. Ecol. Model. 113, 201–223.
Teague, W.R., Foy, J.K., 2002. Validation of SPUR2.4 rangeland simulation model using a cow-calf field experiment. Agric. Syst. 74, 287–302.
Vescovo, L., Gianelle, D., 2006. Mapping the green herbage ratio of grasslands using both aerial and satellite-derived spectral reflectance. Agric. Ecosyst. Environ. 115, 141–149.
Vescovo, L., Gianelle, D., 2008. Using the MIR bands in vegetation indices for the estimation of grassland biophysical parameters from satellite remote sensing in the Alps region of Trentino (Italy). Adv. Space Res. 41, 1764–1772.
Wang, X., Liu, S.J., Zhang, X.W., Hao, L.Z., Zhao, Y.P., Wang, W.B., 2013. Alpine grassland nutrition dynamic monitoring using HJ-1A/1B data. Remote Sens. Land Res. 25, 183–188.
Yan, L., Zhou, G.S., Zhang, F., Sui, X.H., Ping, X.Y., 2012. Spatial heterogeneity of vegetation coverage and its temporal dynamics in desert steppe, Inner Mongolia. Acta Ecol. Sin. 32 (13), 4017–4024.
Zhang, J., Romo, J.T., 1994. Defoliation of a northern wheatgrass community: above- and below-ground phytomass productivity. J. Range Manage. 47, 279–284.